Science and Technology Indonesia
e-ISSN:2580-4391 *p*-ISSN:2580-4405
Vol. 10, No. 2, April 2025

Research Paper

Synergistic Effects of Double Oxidation on the Extraction and Characterization of Crystalline Nanocellulose from Rattan Waste and Kenaf Fiber

Noorasikin Samat[1*], Muhamad Aliff Redhwan Mohamad Roshidi[1], Dona Nur Afiqah Don Ramlan Onn[1], Maziati Akmal Mohd Hatta[2], Fatimah A'thiyah Sabaruddin[3]

[1]*Department of Manufacturing and Materials Engineering, International Islamic University Malaysia (IIUM), Jalan Gombak, Gombak, Kuala Lumpur, 53100, Malaysia*
[2]*Department of Science in Engineering, International Islamic University Malaysia (IIUM), Jalan Gombak, Gombak, Kuala Lumpur, 53100, Malaysia*
[3]*Faculty of Biotechnology and Biomolecular Science, Universiti Putra Malaysia (UPM), Serdang Selangor, 43400, Malaysia*
*__Corresponding author__: noorasikin@iium.edu.my

Abstract
This study investigates the potential of rattan fiber, a by-product of the furniture industry, as a feedstock for nanocellulose production. Cellulose nanocrystals (CNC) were extracted using a double oxidation process that combined bleaching with ammonium persulfate (APS) treatment. The effects of APS reaction time, pre-treatment with and without bleaching, on the crystallinity and morphology of CNC were evaluated. Additionally, the feasibility of applying this extraction method to agro-industrial kenaf fiber was assessed. Fourier transform infrared (FTIR) spectroscopic confirmed the removal of lignin and hemicellulose, while the X-ray diffraction (XRD) analysis showed a gradual increase in the crystallinity index (CrI) of CNCs extracted from rattan and kenaf, achieving 73.40% and 72.40, respectively. Scanning Electron Microscope (SEM) revealed fiber disintegration and Transmission Electron Microscopy (TEM) confirmed the spherical CNCs of rattan and kenaf having a diameter of 61.51 ± 6.46 nm and 31.76 ± 6.34 nm, respectively. Atomic force microscopy (AFM) further indicated smaller CNC sizes in kenaf compared to rattan. These findings suggest that rattan fiber is a promising renewable feedstock for producing nanocellulose, with potential application in various industries.

Keywords
Nanocellulose, AFM, Oxidation, FTIR, Rattan, Kenaf

Received: 27 November 2024, Accepted: 31 January 2025
https://doi.org/10.26554/sti.2025.10.2.411-419

1. INTRODUCTION

Nanocellulose (NC) is a natural carbohydrate polymer that is commonly extracted either from plants or plant residue. Besides having low density, high aspect ratio, and high stiffness, it is also non-toxic and biodegradable. With the growing concerns over global climate change and sustainability, the use of cellulose and NC in the production of sustainable, green-based products with reduced environmental impact has become increasingly important. NC can be generally categorized into three types based on its morphological features and sources including cellulose nanofibrils (CNF), cellulose nanocrystals (CNC), and bacterial nanocellulose (BNC). CNF and CNC are derived from plant-based feedstock and differ mainly in their processing methods and structure. CNF is typically produced through mechanical fibrillation, resulting in long, entangled fiber whereas CNC is obtained through chemical or chemo-mechanical processes (Dungani et al., 2024), yielding shorter, rod-like crystals. BNC on the other hand, is synthesized by certain bacteria, producing pure nanocellulose with unique properties such as a highly porous network structure. Notably, each type of nanocellulose has distinct applications based on its structural characteristics (Razab et al., 2022; Vu et al., 2024; Nasrudin et al., 2022; Nechyporchuk et al., 2016; Rana et al., 2021). To date, cellulose nanocrystals (CNC) also known as NCC have received high attraction from academicians and industrialists due to their versatility in applications. CNCs exhibit significant potential across various fields due to their remarkable mechanical properties, high Young's modulus, tuneable surface characteristic, liquid crystal behaviour, and biocompatibility (Vu et al., 2024).

Numerous sources are available for the production of cellulose and nanocellulose which can be found in plants, animals, fungi, and bacteria. Natural resources like kapok (Rahmatullah et al., 2022; Mi'rajunnisa et al., 2023) and agricultural residues such as jute (Syazwani et al., 2022), various types of oil palm fiber (Al-Dulaimi and Wan Rosli, 2017; Megashah et al., 2018; Padzil et al., 2020; Nasrudin et al., 2022), pineapple leaf (Balakrishnan et al., 2018; Nasrudin et al., 2022), and

many other biomasses serve as viable sources for cellulose production. Kenaf (*Hibiscus cannabinus* L.) is another significant source of natural fibers, widely cultivated as an industrial crop in many countries due to its economic benefits. Known for its fast growth and high yield, kenaf requires minimal water and fertilizers, making it a preferred material. Kenaf also possesses excellent tensile strength and biodegradability which make it a sustainable alternative to synthetic fibers (Song et al., 2018). In contrast, rattan is a forestry resource that is classified as a non-timber forest product. This climbing palm tree is important in the cane furniture industry (Astari et al., 2019; Toni and Mahzan, 2021), and it is predominantly found in southeast Asia region including Vietnam, Indonesia, Philippines, Malaysia and other tropical countries (Wahab et al., 2019). Residual rattan from furniture production holds potential as a source of nanocellulose (NC) feedstock, which can be converted into value-added products. This includes applications in eco-composites, which could generate significant economic benefits.

Two primary approaches can be utilized to extract the CNC namely, the mechanical and chemical methods. According to Zhang et al. (2016), the mechanical method is highly energy-intensive, making it less environmentally friendly. Consequently, many researchers have turned to chemical or combined mechanical–chemical methods, which offer lower energy consumption and yield CNC with higher crystallinity than the mechanical method. Among chemical methods, ammonium persulfate (APS) treatment has emerged as a promising alternative to acid hydrolysis. It is a simpler process and poses a lower long-term environmental toxicity risk (Cheng et al., 2014; Nascimento et al., 2016). While APS treatment offers the advantage of being a one-step method, it does require an extended treatment time of approximately 16 hours (Oun and Rhim, 2017; Khanjanzadeh and Park, 2020).

In response to this limitation, our previous work demonstrated that the CNCs were successfully extracted from the EFB fibre and pineapple leaves with a shortened APS treatment time of 9 hours (Nasrudin et al., 2022). The extracted CNCs exhibited differences in particle size and morphology, including both spherical and rod-like shapes. The study also found that pretreatment with bleaching facilitates easier defibrillation during subsequent APS treatment. Therefore, the double oxidation approach; combining bleaching and APS treatments, offers an effective alternative for CNC extraction in a shorter time.

In the present work, the rattan powder, a by-product from mill waste, was evaluated as a raw material for producing CNC using combined bleaching and APS treatments. The APS treatment time after bleaching was varied and compared with the APS treatment time without bleaching. The chemical composition, morphology, and crystallinity of the obtained CNC were characterized using FTIR analysis, SEM and TEM, AFM, and XRD. The efficiency of the combined treatment in producing CNC from rattan was further compared with that of agro-industrial kenaf fiber, providing insight into the effectiveness of these processes across different biomass sources.

2. EXPERIMENTAL SECTION

2.1 Materials

Rattan waste in powder form and kenaf fiber was supplied by Rinaat Cane Sdn. Bhd, Perak, Malaysia and Lembaga Kenaf dan Tembakau Negara (LKTN), Kelantan, Malaysia, respectively. The fibers were dried, crushed, ground, and sieved using a 45-μm mesh. Sodium chlorite ($NaClO_2$), acetic acid (CH_3COOH), APS in pellet form were purchased from Morning Prestige Trading Sdn Bhd, Malaysia. The instruments used for analysis include Fourier transform infrared spectroscopy (FTIR)(Bruker, Invenio), Scanning electron microscopy (SEM) (JOEL,JSM-5600), Transmission electron microscopy (TEM)(H7650 Hitachi Ltd.), Atomic Force Microscopy (AFM) (NanoWizard II), X-ray diffraction (XRD) (Bruker, D2 Phaser) and Freeze-Drying (Buchi, Lyovapor L-200).

2.2 Methods

2.2.1 Nanocellulose Preparation

The combined treatment of CNC extraction is in accordance with the work by Nasrudin et al. (2022). For the bleaching treatment, a 0.7% (w/v) $NaClO_2$ solution was prepared and acetic acid was added slowly until the solution reached pH 4. The dried and ground rattan powder and kenaf fiber were added to the $NaClO_2$ solution, stirred and heated to 80 °C for 2 hours to bleach the fibers. The bleaching steps were repeated several times until the suspension appeared white. The residue was then washed with distilled water to remove lignin and hemicellulose, and until it reached the pH 4, and finally oven-dried at 70 °C. In the direct treatment, the bleaching step was skipped. For the APS treatment, a constant concentration of 1 M APS solution was used. After preparing the solution the fiber was immersed in it. The APS mixture was then heated at 80 °C and stirred for 9 and 16 hours. The oxidized fibers were centrifuged at 5000 rpm and was washed adequately until the pH value reached 4. The CNC aqueous suspension was sonicated in an ice bath for 30 mins, followed by freeze-drying for 4 days. Figure 1 shows the steps involved in this work and Table 1 summarizes the treatment and fiber notations used in the current work.

2.2.2 Characterizations

The crystallinity pattern of the obtained cellulose was analyzed using X-ray diffractometer (Bruker, D2 Phaser), The samples were recorded from 10° to 40° (2θ) using 0.02° step mode with a scan rate of 37 s/step. The crystallinity index (CrI) of the samples after XRD analysis was calculated using an Equation as follows (Segal et al., 1959):

$$CRI(\%) = \left[\frac{I_{200} - I_{am}}{I_{am}}\right] \times 100$$

where, I_{200} and I_{am} is the intensity of close to 22.5° and amorphous around 18.5°, respectively. The functional group

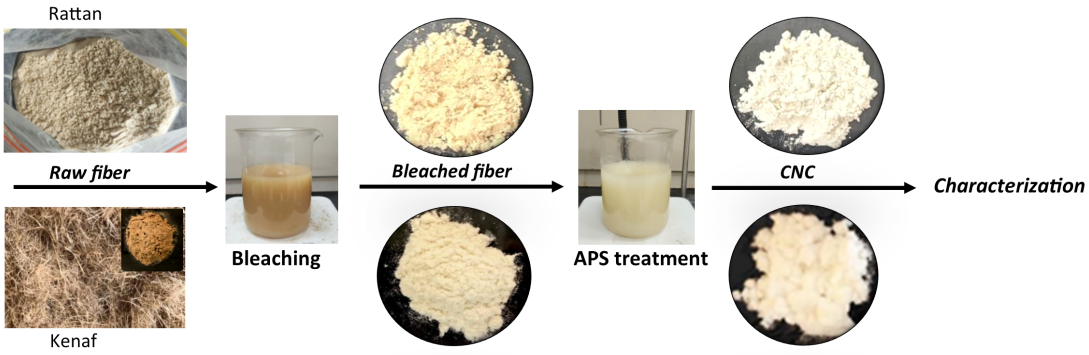

Figure 1. The Schematic Diagram of CNC Extraction Process

analysis of raw, bleached, and APS treatment samples was conducted using the FTIR spectrometer (Bruker, Invenio) with a resolution of 4 cm^{-1} and 16-64 scans in the spectral range of 4000-400 cm^{-1}. AFM was employed to characterize the topography of the CNCs. Measurements were performed in tapping mode using AFM (NanoWizard II). For sample preparation, a drop of diluted aqueous suspension (sonicated) of CNC was dispersed onto the surface of an optical glass substrate and allowed to dry at ambient temperature before transferring the samples to the AFM instrument.

The morphologies of samples were analyzed using SEM (JOEL, JSM-5600) operating at 7 kV. The samples were coated with palladium using an auto fine-coater (Quorum Tech. SC7-620 Mini Sputter Coater). Additionally, the CNC images were obtained using TEM (H7650 Hitachi Ltd.), operating at 200 kV. The CNC suspension (0.01%) was stained with a 3.0 wt% solution of phosphotungstic acid for 2 mins and then dried at room temperature. The CNC dimension were estimated using an image analysis (ImageJ software).

Table 1. Notation of Rattan and Kenaf Samples

Samples	Bleaching Treatment	APS Treatment Time (hr)
r_Rtn	N	N
B-Rtn	Y	N
B-Rtn/APS9	Y	9
B-Rtn/APS16	Y	16
r_Rtn/APS9	N	9
r_Rtn/APS16	N	16
r_Knf	N	N
B-Knf	Y	N
B-Knf/APS9	Y	9
B-Knf/APS16	Y	16
r_Knf/APS9	N	9
r_Knf/APS16	N	16

**Rtn = rattan; Knf = kenaf; Y = Yes; N = No*

3. RESULTS AND DISCUSSION

3.1 Chemical Composition Analysis

The FTIR spectra of rattan and kenaf fiber before and after bleaching and APS treatment are shown in Figure 2, illustrating the changes in their chemical structures. It can be observed that the FTIR spectra of raw rattan and kenaf fibers, as shown in Figures 2(a) and (b), exhibit nearly identical absorption peaks, with slight variations in wavelength values and peak intensities. These differences can be attributed to variations in the content of hemicellulose, lignin, and cellulose. The chemical compositions of rattan (Zuraida et al., 2015) and kenaf (Khalil et al., 2010) fibers prior to APS treatment are summarized in Table 2 (The rattan and kenaf fibers examined in these studies originated from the same source as those used in the present study). The essential features of the cellulosic profile in all samples are evident at higher wavelengths, characterized by a broad absorption peak of 3329 cm^{-1}, and another peak in the range of 2892 - 2900 cm^{-1}. These bands belong to the stretching vibrations of hydrogen bonds in O–Hand C–H groups, respectively (Samat et al., 2021; Mi'rajunnisa et al., 2023).

For the non-cellulosic components (lignin and hemicellulose), the primary peaks at 1733 - 1736 cm^{-1}, are associated with the stretching of acetyl group (C=O) in hemicellulose or carboxylic acid in lignin. These peaks decreased significantly after bleaching. Nevertheless, this adsorption peak maintained after the APS treatment, indicating the presence of carboxylic acid groups on the fiber surface as a result of the APS carboxylation reaction (Samat et al., 2022). It is noticed that the peak near 1510 - 1515 cm^{-1}, which assigned to the C=C stretching vibrations of the aromatic rings of lignin, disappeared after the bleaching, suggesting the occurrence of delignification which led to lignin removal. Similar findings were reported by Sabaruddin et al. (2021), where a significant reduction in lignin content was observed following the bleaching treatment, with over 98% of lignin removed compared to the raw sample. In their study, both bleaching and acid hydrolysis were employed to extract nanocellulose from the kenaf core, demonstrating the effectiveness of these methods.

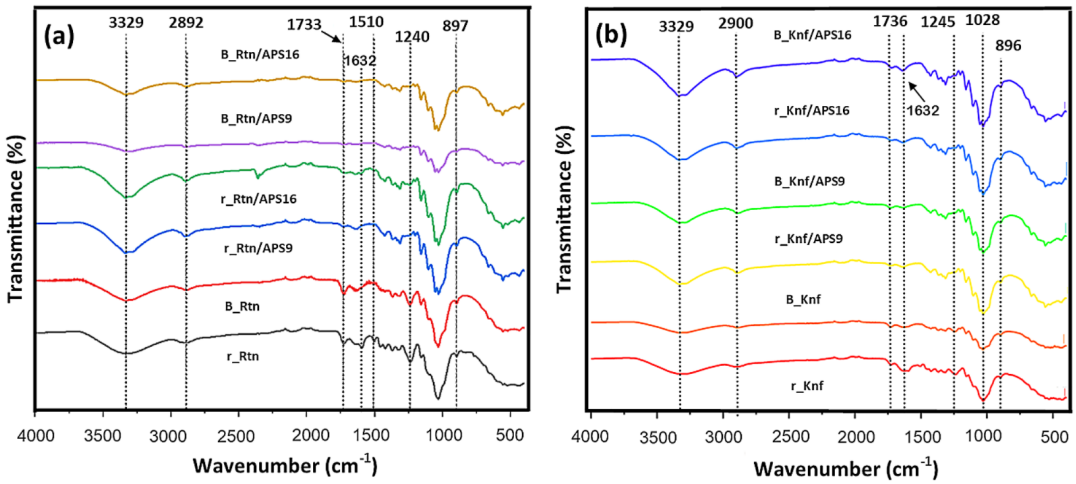

Figure 2. FTIR Spectra of (a) Rattan Fibers, and (b) Kenaf Fibers

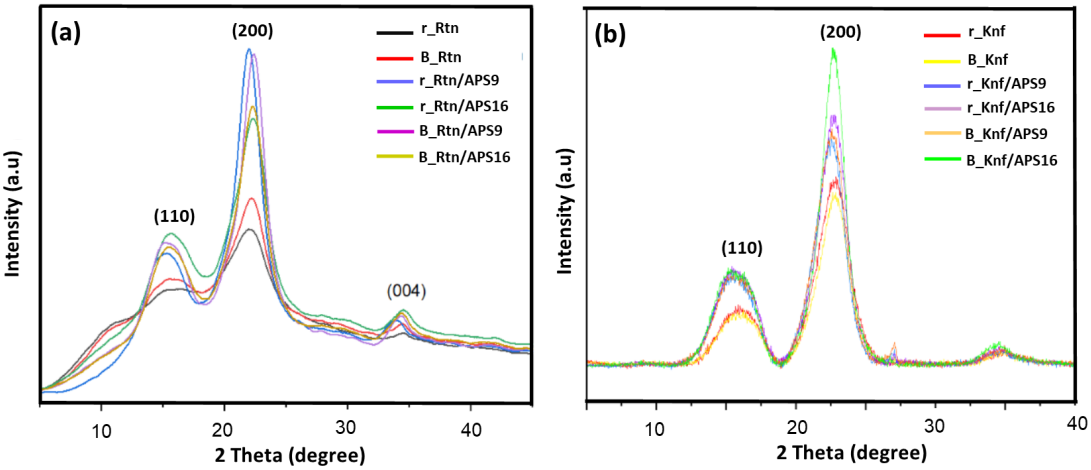

Figure 3. XRD Diffractograms for (a) Rattan Fibers, and (b) Kenaf Fibers

Next characteristics located at 1240-1245 cm^{-1}, which refers to −COO of acetyl group in the hemicellulose, shows a lower peak intensity after subjected to bleaching treatment. The decreasing peak indicates a partial elimination of hemicellulose, and the results suggest that the bleaching treatment alone was insufficient to completely remove the hemicellulose. According to Wahib et al. (2022), the removal of hemicellulose was slightly lower than that of lignin after the bleaching treatment, with 90% and 97%, respectively. In their study, they employed the bleaching treatment along with the mechanical stirrer method (CNCs1) and Soxhlet apparatus method (CNCs2) to extract CNC from date pit.

It is worth noting that the subsequent treatment of bleached samples with APS further eliminated the residual hemicellulose content, as these peaks are no longer observed. Moreover, the transformation of the bleached fiber's color from brown to a whitening appearance after APS treatment (Figure 1) further supports the absence of non-cellulosic components. Another important feature of carbohydrates adsorptions peaks is the prominent peak at 1030 cm^{-1}, corresponding to the bending vibration of C–O–C pyranose ring. Meanwhile, a minor peak observed at 896–897 cm^{-1} is assigned to the β (1-4) glycosidic linkage of glucose units in rattan and kenaf cellulose. The existence of these peaks, along with the broad OH (3300 cm^{-1}) and CH (2900 $cm^{-}1$) peaks in all samples, including the raw fiber and CNC, implies that the applied treatments did not alter the structure of NC. On the other hand, for the effect of direct treatment (without bleaching), regardless of the APS treatment time (9 and 16 hours), the FTIR spectrum of CNC for rattan and kenaf is indistinguishable, and only minor differences in peak intensity were observed.

Table 2. Chemical Composition of Rattan and Kenaf Fiber

Fiber/Composition (%)	Extractive	Hollocellulose	Cellulose	Hemicellulose	Lignin	Ash
Rattan (Zuraida et al., 2015)	-	-	34.3	45.6	21	5.4
Kenaf (Khalil et al., 2010)	5.5	86.8	55	-	14.7	5.4

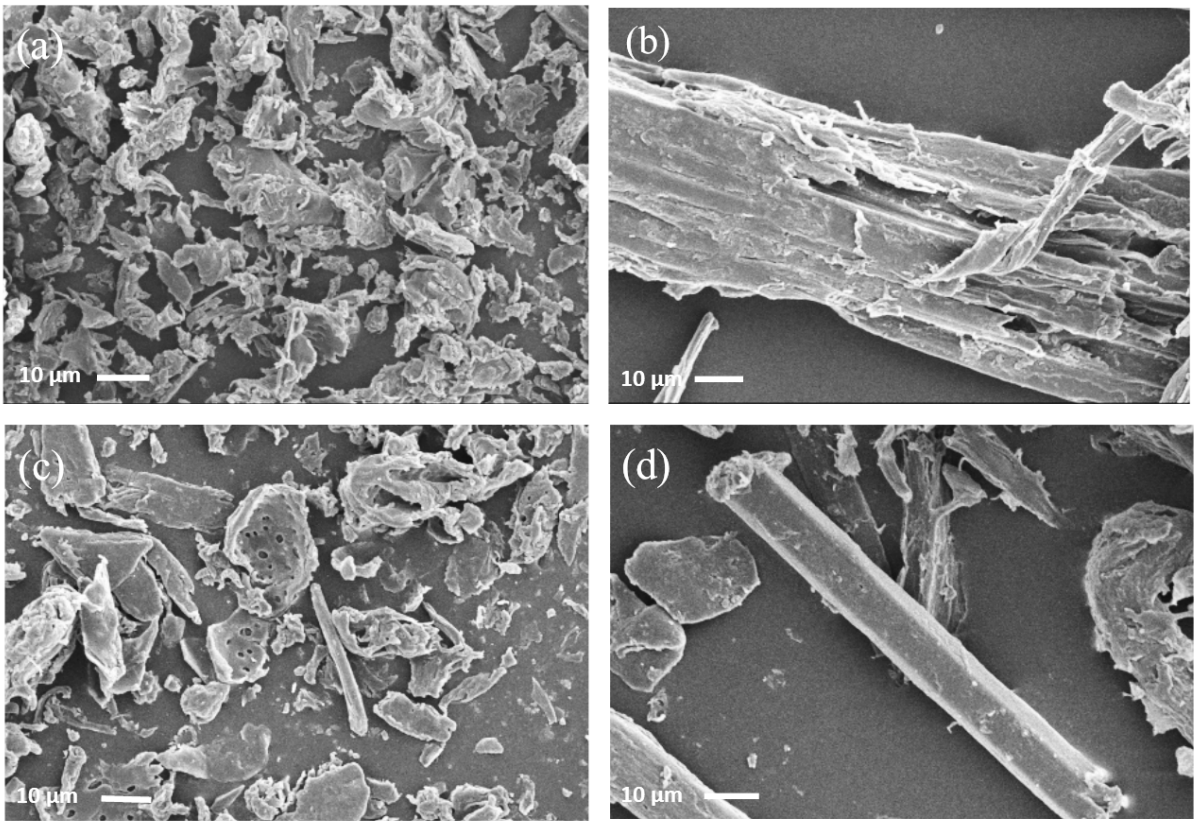

Figure 4. SEM Micrographs of (a-b) Raw, and (c-d) Bleached Samples, of Rattan and kenaf Fibers, Respectively

3.2 Crystallinity Analysis

The XRD spectral patterns for rattan and kenaf samples is presented in Figure 3, illustrating the crystallinity properties before and after the treatments. All samples demonstrate several distinct diffraction peaks, which are indexed as cellulose I at 2θ = 13.3°–17.4° (110), 18.7°–24.4° (200), and 22.5°–35.7° (004). As depicted in the XRD diffractometer, the existence of a new peak was not noticeable. Indeed, the introduction of bleaching and APS treatment can affect the peak shape characteristic in terms of intensity and broadness/sharpness. In general, the peak intensity increased, and the peaks appeared sharper after the combined treatments, which is related to the elimination of hemicellulose and lignin from the raw fibers. As the lignin and hemicellulose are amorphous components, their elimination allows for more organized cellulose chains, resulting in a higher degree of crystallinity, as reflected in the sharper XRD peaks (Montoya-Escobar et al., 2022; Aisy et al., 2024).

The crystallinity index (CrI) for all samples is summarized in Table 3. The bleaching treatment of raw rattan and kenaf fibers improved their CrI values, increasing from 40.86% to 50.23% for rattan and from 66.76% to 69.53% for kenaf. This increase indicates better crystallinity in the bleached fibers compared to the raw fiber samples, which is attributed to the partial removal of lignin and hemicellulose. The following treatment of the bleached rattan and kenaf samples with APS for 9-hour resulted in further removal of non-cellulosic components, leading to an even higher degree of crystallinity, with CrI values reaching 73.4% and 72.4%, respectively.

Overall, the increase in the CrI value observed in the combined treatments (with 9-hour APS) was more pronounced in the CNC extracted from rattan, showing a twofold increase compared to the CNC extracted from kenaf. These results indicate significant enhancement in the crystallinity of rattan fiber

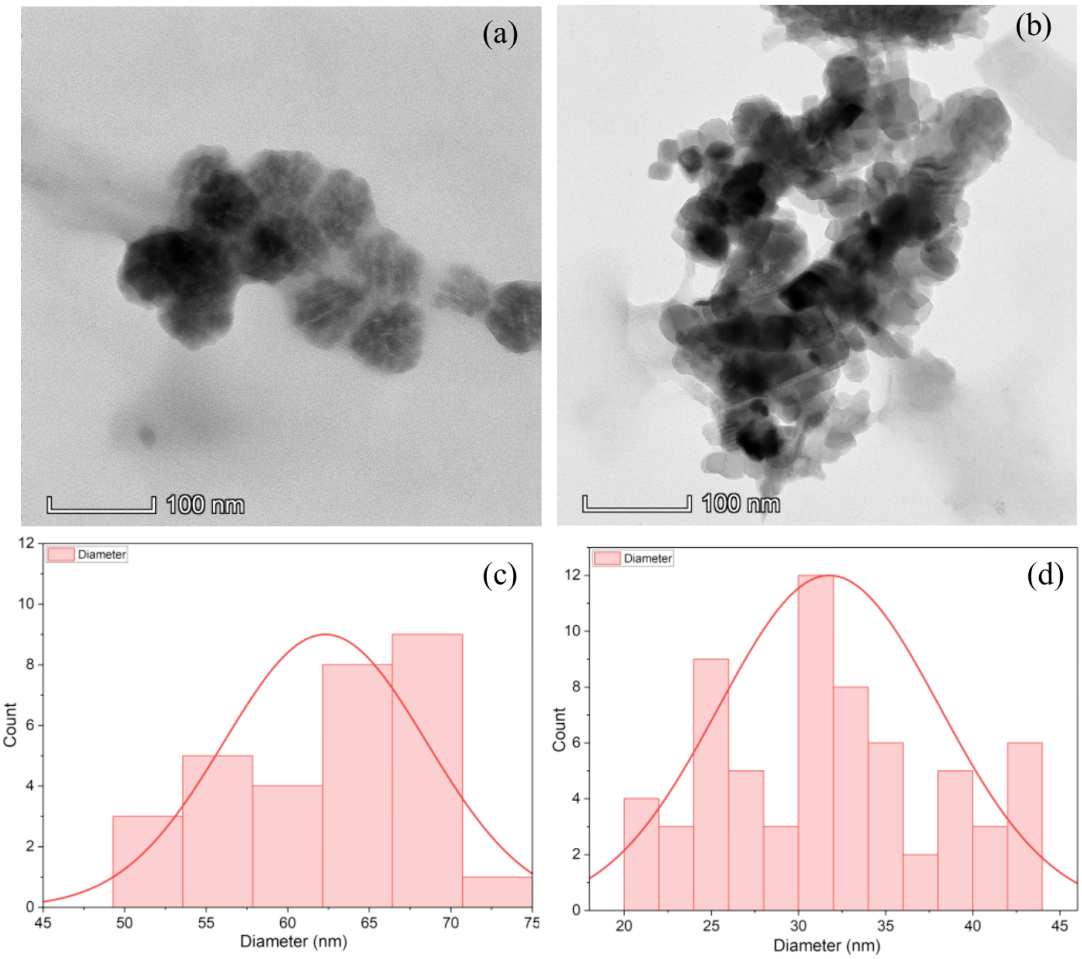

Figure 5. TEM Micrographs of CNC and Its Distribution for (a,c) Rattan; and (b,d) Kenaf

Table 3. Summary of The Crystallinity Index (CrI) for All Samples

Samples	I(200)	Iam	CrI (%)
r_Rtn	63.09	37.29	40.89
B-Rtn	74.58	37.12	50.23
B-Rtn/APS9	127.02	33.79	73.40
B-Rtn/APS16	106.71	34.79	67.40
r-Rtn/APS9	127.18	34.13	73.16
r_Rtn/APS16	103.04	42.12	59.12
r-Knf	141.04	46.88	66.76
B-Knf	127.24	38.77	69.53
B-Knf/APS9	173.36	47.84	72.4
B-Knf/APS16	206.10	38.80	81.17
r-Knf/APS9	165.27	51.42	68.89
r-Knf/APS16	171.47	53.52	68.79

as a result of the treatment process. However, extending the APS treatment time to 16 hours produced an opposite trend. For rattan, the CrI decreased from 73.4% to 67.4%, while for kenaf, the CrI continued to increase; reaching 81.17%. As shown in Table 3, for rattan samples without bleaching, the 9-hour APS treatment improved the CrI significantly, increasing it from 40.86% to 73.16%. Interestingly, the CrI values for bleached and unbleached rattan samples treated with APS for 9 hours were nearly identical (73.4% and 73.16%, respectively). In contrast, extending the APS treatment time to 16 hours caused the CrI of the rattan sample to decrease to 59.12%. This reduction suggests that prolonged APS treatment led to degradation in the crystalline regions of the rattan macromolecules. These findings imply that extending the APS treatment duration beyond 9 hours is not only ineffective for extracting CNC from rattan fiber but may also be detrimental to its crystalline structure.

Unlike rattan fiber, the CrI of kenaf fiber without bleaching was not significantly affected by the treatment time, as the values were quite similar regardless of whether the kenaf fiber was immersed for 9 or 16 hours (68.89% and 68.79%, respectively). These results suggest that the removal of non-cellulosic components from kenaf fiber is more efficient via the combined treatment compared to direct APS treatment. Similar findings

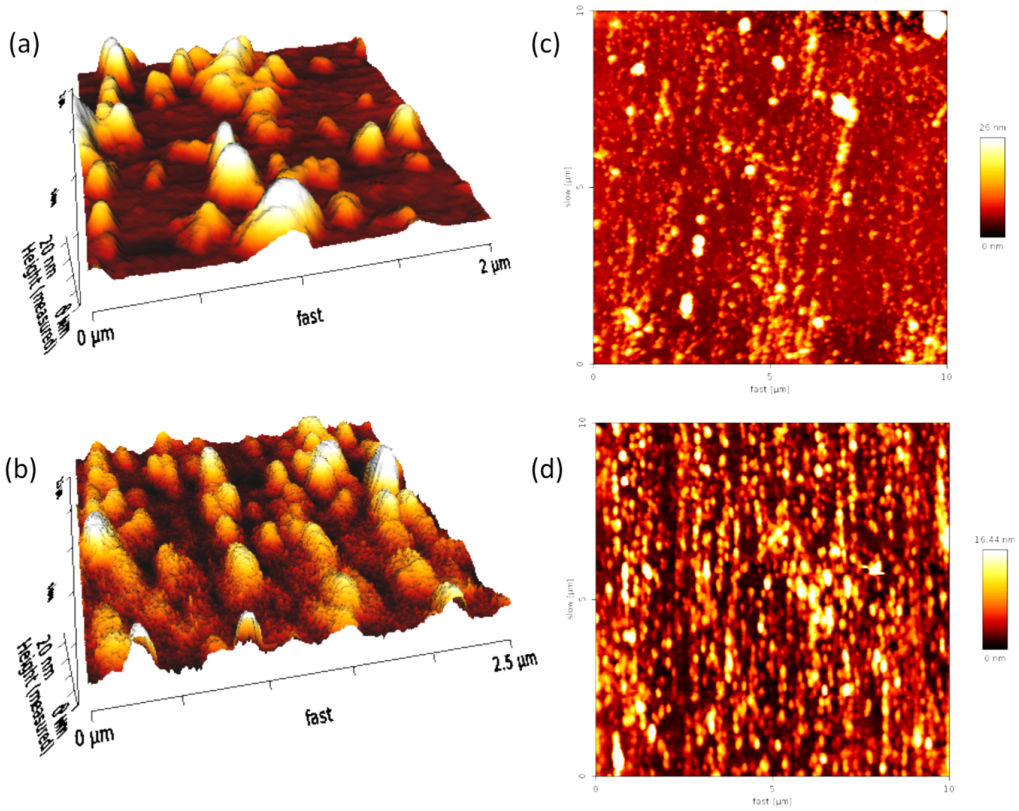

Figure 6. AFM Images of CNC of (a,c) Rattan, and (b,d) Kenaf Fibers

were also reported by Sabaruddin et al. (2021) in their work on the isolation of kenaf nanocrsytalline cellulose (NCC) from kenaf core through bleaching and acid hydrolysis. They found that the bleaching process effectively removed non-cellulosic components, including lignin and hemicellulose, which led to an increase in the crystallinity of the NCC.

3.3 Morphological Analysis

The morphological analysis of rattan and kenaf fibers was conducted using SEM, the results are presented in Figure 4. For the raw samples, rattan fibers appear as irregular round shapes, while while kenaf fibers exhibit a long, shape, as shown in Figures 4(a) and (b), respectively. A rough surface characteristic which is attributed to the presence of non-cellulosic components (lignin, pectin, and hemicellulose) are evident in Figures 4(a) and (b). Similar observations were reported by Ding et al. (2022) and Sulaiman et al. (2015), who suggested that the high surface roughness in raw sample indicates the presence of non-cellulosic components, including lignin and hemicellulose. Additionally, the microfibrils, which exist in bundled form, can be seen in Figure 4(b). The results of the bleaching treatment, depicted in Figures 4(c) and (d), show that the fiber surfaces were smoother, which corresponds to the partial removal of hemicellulose and lignin. Moreover, the width of rattan and kenaf fibre was relatively smaller than before bleaching, 23.45 ± 3.28 and 14.18 ± 0.753 μm, respectively.

The efficient interaction of the bleached fiber with 9-hour APS treatment for the CNC extraction was confirmed through TEM characterization. The observation of TEM micrographs in Figure 5 show that the extracted CNCs exist in a spherical shape. It is also noticed that the CNCs of rattan (Figure 5(a)) appeared larger than those from kenaf (Figure 5(b)). Additionally, the diameter distribution of CNCs, as determined from TEM micrographs, is shown in Figures 5(c) and (d). A narrow diameter distribution is evident, with CNCs from rattan ranging from 48 - 75 nm and CNCs from kenaf ranging from 20 - 45 nm. Based on this analysis, the average diameters of CNCs extracted from rattan and kenaf are 61.51 ± 6.46 nm and 31.76 ± 6.34 nm, respectively. This study successfully extracted CNCs from different lignocellulosic sources which are non-timber forest fiber (rattan) and industrial crop fiber (kenaf). These results are in consistent with those reported in our previous work (Nasrudin et al., 2022), which utilized the combined or double oxidation treatments to extract the CNC from EFB and pineapple leaf. Although the APS treatment time was 9 hr, it was sufficient to produce the CNC. Certainly, the pre-treatment with bleaching proved to be an essential step to promote the defibrillation process during the oxidation

reaction with APS.

The morphology of the extracted CNC was also characterized by conducting the AFM analyses. Figures 6 (a) and (b) present the AFM topography images based on height factor. The images reveal the presence of bright and dark regions in the form of round or spherical shapes. The larger spherical shape observed for rattan in Figure 6(a) aligns well with the corresponding TEM micrograph. In addition, te bright regions indicate the presence of crystalline areas, while the dark spots reflect amorphous regions along the fiber axis within the CNCs. As seen in Figures 6 (a) and (b), the bright region encompassed a quite large area in both CNCs type, which implies high crystallinity (CrI of rattan and kenaf =>70%).

In AFM, the root mean square (RMS) roughness (Rq) refers to the square root of the distribution of surface height on the NC film, or in this case the height of CNC on the glass substrate. A low Rq value indicates low surface roughness or a smooth surface. From Figures 6 (c) and (d), the Rq values are as follows: Rq (rattan = 3.181 nm) > Rq (kenaf = 2.956 nm). According to Shanmugam et al. (2023), the surface roughness of CNF film is determined by the diameter and the aspect ratio of the NC, where smaller fiber diameter results in lower roughness. Hence, it is likely that the homogenous and high aspect ratio of the produced CNC contributed to the smooth surface and lower Rq values. Indeed, the spherical CNC extracted in this study demonstrates potential applications not only in food packaging and composite materials but also as a stabilizer for oil-in-water Pickering emulsions. Mikulcová et al. (2018) reported that CNC extracted via APS treatment could effectively form stable oil-in-water emulsions, using triglycerides (tricaprylin/tricaprin) as the oil phase.

4. CONCLUSIONS

The extraction of CNC from rattan and kenaf fibers using double oxidation treatments was successfully carried out. A 9-hour treatment with APS, combined with pre-treatment bleaching, was sufficient to produce CNC. At this optimal treatment time, the CrI values for rattan and kenaf increased to 73.4% and 72.4%, respectively, with a negligible difference. However, at a 16-hour APS treatment time, the CrI for rattan decreased, while it increased for kenaf, likely due to differences in the raw material sources. The TEM morphological feature of both CNC show a spherical shape, which proved that the non-cellulosic components were removed, which is consistent with the FTIR analysis. The findings of this research demonstrate that rattan fibers are a promising feedstock for CNC production, and the double oxidation treatment is an effective method for extracting CNC.

5. ACKNOWLEDGMENT

This research did not receive any specific grant from funding agencies in the public, commercial, or not-for-profit sectors. Authors thank IIUM for the support of this research.

REFERENCES

Aisy, L. A. R., T. Kemala, L. Suryanegara, and H. Purwaningsih (2024). Isolation and Characterization of Cellulose Nanofibrils (CNF) from Dates-by-Product via Citric Acid Hydrolysis. *Science and Technology Indonesia*, **9**(4); 818–827

Al-Dulaimi, A. A. and W. D. Wan Rosli (2017). Isolation and Characterization of Nanocrystalline Cellulose from Totally Chlorine Free Oil Palm Empty Fruit Bunch Pulp. *Journal of Polymers and the Environment*, **25**(2); 427–437

Astari, L., S. Sudarmanto, S. S. Kusumah, F. Akbar, and K. W. Prasetiyo (2019). Quality of Particleboard Made from Rattan Waste. In *IOP Conference Series: Earth and Environmental Science*, volume 374. page 012009

Balakrishnan, P., S. Gopi, V. G. Geethamma, N. Kalarikkal, and S. Thomas (2018). Cellulose Nanofiber vs Nanocrystals from Pineapple Leaf Fiber: A Comparative Study on Reinforcing Efficiency on Starch Nanocomposites. *Macromolecular Symposia*, **380**(1); 1800102

Cheng, M., Z. Qin, Y. Liu, Y. Qin, T. Li, L. Chen, and M. Zhu (2014). Efficient Extraction of Carboxylated Spherical Cellulose Nanocrystals with Narrow Distribution Through Hydrolysis of Lyocell Fibers by Using Ammonium Persulfate as an Oxidant. *Journal of Materials Chemistry A*, **2**(1); 251–258

Ding, L., X. Han, L. Cao, Y. Chen, Z. Ling, J. Han, S. He, and S. Jiang (2022). Characterization of Natural Fiber from Manau Rattan (*Calamus manan*) as a Potential Reinforcement for Polymer-Based Composites. *Journal of Bioresources and Bioproducts*, **7**(3); 190–200

Dungani, R., M. I. Bakshi, T. Z. Hanifa, M. Dew, F. A. Syamani, M. Mahardika, and W. Fatriasari (2024). Isolation and Characterization of Cellulose Nanofiber (CNF) from Kenaf (*Hibiscus cannabinus*) Bast Through the Chemo-Mechanical Process. *Journal of Renewable Materials*, **12**(6); 1057–1069

Khalil, H. P. S. A., A. F. I. Yusra, A. H. Bhat, and M. Jawaid (2010). Cell Wall Ultrastructure, Anatomy, Lignin Distribution, and Chemical Composition of Malaysian Cultivated Kenaf Fiber. *Industrial Crops and Products*, **31**(1); 113–121

Khanjanzadeh, H. and B. D. Park (2020). Characterization of Carboxylated Cellulose Nanocrystals from Recycled Fiberboard Fibers Using Ammonium Persulfate Oxidation. *Journal of the Korean Wood Science and Technology*, **48**(2); 231–244

Megashah, L. N., H. Ariffin, M. R. Zakaria, and M. A. Hassan (2018). Properties of Cellulose Extract from Different Types of Oil Palm Biomass. *IOP Conference Series: Materials Science and Engineering*, **368**(1); 012049

Mikulcová, V., R. Bordes, A. Minarík, and V. Kašpárková (2018). Pickering Oil-In-Water Emulsions Stabilized by Carboxylated Cellulose Nanocrystals—Effect of the pH. *Food Hydrocolloids*, **80**; 60–67

Mi'rajunnisa, H. S., H. Suryadi, Sutriyo, and Y. P. I. Lestari (2023). Isolation of Cellulase from Selected Fungal Strains and Its Use for Manufacture Microcrystal Cellulose from Kapuk Cortex (*Ceiba pentandra* (L.) Gaertn). *Science and Technology Indonesia*, **8**(2); 227–234

Montoya-Escobar, N., D. Ospina-Acero, J. A. Velásquez-Cock, C. Gómez-Hoyos, A. S. Guerra, P. F. G. Rojo, L. M. V. Acosta, J. P. Escobar, N. Correa-Hincapié, O. Triana-Chávez, R. Z. Gallego, and P. M. Stefani (2022). Use of Fourier Series in X-Ray Diffraction (XRD) Analysis and Fourier-Transform Infrared Spectroscopy (FTIR) for Estimation of Crystallinity in Cellulose from Different Sources. *Polymers*, **14**(23); 5199

Nascimento, D. M. D., J. S. Almeida, M. do S. Vale, R. C. Leitão, C. R. Muniz, M. C. B. de Figueirêdo, J. P. S. Morais, and M. de F. Rosa (2016). A Comprehensive Approach for Obtaining Cellulose Nanocrystal from Coconut Fiber. Part I: Proposition of Technological Pathways. *Industrial Crops and Products*, **93**; 66–75

Nasrudin, R. F., N. Samat, N. A. Mokhtar, and N. Yacob (2022). Production of Cellulose Nanocrystals from Oil Palm Empty Fruit Bunch and Pineapple Leaf Fibre Using Double Oxidation Approach. *Jurnal Teknologi*, **84**(5); 73–81

Nechyporchuk, O., M. N. Belgacem, and J. Bras (2016). Production of Cellulose Nanofibrils: A Review of Recent Advances. *Industrial Crops and Products*, **93**; 2–25

Oun, A. A. and J.-W. Rhim (2017). Characterization of Carboxymethyl Cellulose-Based Nanocomposite Films Reinforced with Oxidized Nanocellulose Isolated Using Ammonium Persulfate Method. *Carbohydrate Polymers*, **174**; 484–492

Padzil, F. N. M., S. H. Lee, Z. M. A. Ainun, C. H. Lee, and L. C. Abdullah (2020). Potential of Oil Palm Empty Fruit Bunch Resources in Nanocellulose Hydrogel Production for Versatile Applications: A Review. *Materials*, **13**(5); 1245

Rahmatullah, R., R. W. Putri, M. Rendana, U. Waluyo, and T. Andrianto (2022). Effect of Plasticizer and Concentration on Characteristics of Bioplastic Based on Cellulose Acetate from Kapok (*Ceiba pentandra*) Fiber. *Science and Technology Indonesia*, **7**(1); 73–83

Rana, A. K., E. Frollini, and V. K. Thakur (2021). Cellulose Nanocrystals: Pretreatments, Preparation Strategies, and Surface Functionalization. *International Journal of Biological Macromolecules*, **182**; 1554–1581

Razab, M. K. A. A., R. S. M. Ghani, F. A. M. Zin, N. A. A. N. Yusoff, and A. M. Noor (2022). Isolation and Characterization of Cellulose Nanofibrils from Banana Pseudostem, Oil Palm Trunk, and Kenaf Bast Fibers Using Chemicals and High-Intensity Ultrasonication. *Journal of Natural Fibers*, **19**(13); 5537–5550

Sabaruddin, F. A., P. M. Tahir, S. M. Sapuan, R. A. Ilyas, S. H. Lee, K. Abdan, N. Mazlan, A. S. M. Roseley, and H. P. S. A. Khalil (2021). The Effects of Unbleached and Bleached Nanocellulose on the Thermal and Flammability of Polypropylene-Reinforced Kenaf Core Hybrid Polymer Bionanocomposites. *Polymers*, **13**(1); 1–19

Samat, N., R. F. Nasrudin, and N. S. Engliman (2022). Fabrication of Poly(vinyl) Alcohol-Cellulose Nanocrystal Hybrid Aerogel. *Materials Science Forum*, **1074**; 11–16

Samat, N., M. A. Sulaiman, Z. Ahmad, and H. Anuar (2021). A Comparative Study on the Desiccant Effect of Polypropylene and Polylactic Acid Composites Reinforced with Different Lignocellulosic Fibres. *Journal of Applied Science and Engineering*, **24**(2); 223–231

Segal, L., J. J. Creely, A. E. Martin Jr, and C. M. Conrad (1959). An Empirical Method for Estimating the Degree of Crystallinity of Native Cellulose Using the X-Ray Diffractometer. *Textile Research Journal*, **29**(10); 786–794

Shanmugam, K., N. Chandrasekar, and R. Balaji (2023). Barrier Performance of Spray Coated Cellulose Nanofibre Film. *Micro*, **3**(1); 192–207

Song, Y., W. Jiang, Y. Zhang, H. Wang, F. Zou, K. Yu, and G. Han (2018). A Novel Process of Nanocellulose Extraction from Kenaf Bast. *Materials Research Express*, **5**(8); 085032

Sulaiman, S., M. N. Mokhtar, M. N. Naim, A. S. Baharuddin, M. A. M. Salleh, and A. Sulaiman (2015). Study on the Preparation of Cellulose Nanofibre (CNF) from Kenaf Bast Fibre for Enzyme Immobilization Application. *Sains Malaysiana*, **44**(11); 1541–1550

Syazwani, N. S., M. N. E. Efzan, C. K. Kok, and M. J. Nurhidayatullaili (2022). Analysis on Extracted Jute Cellulose Nanofibers by Fourier Transform Infrared and X-Ray Diffraction. *Journal of Building Engineering*, **48**; 103744

Toni, N. M. M. and S. Mahzan (2021). Influences of Chemical Treatment on Mechanical Properties of Rattan. *Research Progress in Mechanical and Manufacturing Engineering*, **2**(2); 590–598

Vu, A. N., L. H. Nguyen, K. Yoshimura, T. D. Tran, and H. V. Le (2024). Cellulose Nanocrystals Isolated from Sugarcane Bagasse Using the Formic/Peroxyformic Acid Process: Structural, Chemical, and Thermal Properties. *Arabian Journal of Chemistry*, **17**(8); 105841

Wahab, R., N. Mokhtar, R. S. Mohd Ghani, and M. S. Sulaiman (2019). An Overview of Rattan Industry Status and Its Economic Aspect in Setting Up Rattan-Based Industry in Malaysia. *e-BANGI: Jurnal Sains Sosial dan Kemanusiaan*, **16**(3); 1–10

Wahib, S. A., D. A. Da'na, and M. A. Al-Ghouti (2022). Insight into the Extraction and Characterization of Cellulose Nanocrystals from Date Pits. *Arabian Journal of Chemistry*, **15**(3); 103650

Zhang, K., P. Sun, H. Liu, S. Shang, J. Song, and D. Wang (2016). Extraction and Comparison of Carboxylated Cellulose Nanocrystals from Bleached Sugarcane Bagasse Pulp Using Two Different Oxidation Methods. *Carbohydrate Polymers*, **138**; 237–243

Zuraida, A., T. Maisarah, A. Zahurin, A. M. Luqman, R. Wan Yussof, W. Wan Shazlin Maisarah, and A. Marjan (2015). Structural Examination and Elemental Composition Analysis of Rattan Waste Fibers for Binderless Board Application. *Malaysian Journal of Microscopy*, **11**; 39–44

